

ABELL 754: A NON-HEAD ON COLLISION OF SUBCLUSTERS

Mark J. Henriksen

Department of Physics, University of North Dakota , Grand Forks, ND 58202-7129

E-mail: mahenrik@plains.NoDak.edu

and

Maxim L. Markevitch¹

Department of Astronomy, University of Virginia , Charlottesville, VA 22903-0818

E-mail: mlm5y@virginia.edu

Submitted to *The ApJ Letters*, 1995 April 15

ABSTRACT

We have analyzed spatially resolved spectra of the A754 cluster of galaxies obtained with ASCA. Through earlier observations with HEAO-1, Einstein, and ROSAT as well as optical studies, A754 has been established as the prototype system for a merger in progress. The combination of spectral and spatial resolution over a broad energy band provided by ASCA has set unprecedented constraints on the hydrodynamical effects of a cluster merger. We find significant gas temperature variations over the cluster face, indicating shock heating of the atmosphere during the merger. The hottest region, > 12 keV (90% confidence), is located in the region of the Northwest Galaxy clump though the entire region along the cluster axis appears to be hotter than the mean cluster temperature (~ 9 keV). The cool, ≤ 5 keV, gas originally found with the HEAO1-A2 experiment, resides in the exterior of the cluster atmosphere and in plume of gas we identify with a stripped cool atmosphere of the infalling subcluster. We have also attempted to reconstruct an iron abundance map of this merging system. Though poorly constrained, no significant deviations of abundance from the mean value are apparent in the individual regions.

A754 is the only cluster so far which shows the significant temperature pattern expected in a subcluster merger, in both the ROSAT (Henry & Briel 1995) and ASCA data, providing the first possibility to compare it with theoretical predictions. The cluster does not feature a hot peak accompanied by two hot lobes perpendicular to the cluster axis, predicted by hydrodynamic simulations of a head-on merger. The observed temperature and surface brightness maps suggest that the two colliding subunits have missed each other by about 1 Mpc, and are now moving perpendicular to the cluster axis in the image plane (as, e.g., in the simulations by Evrard et al. 1996).

Subject headings: galaxies: clusters: individual (A754) — intergalactic medium — X-rays: galaxies

1. Introduction

A754, a rich hot cluster of galaxies at $z = 0.0541$ (Bird 1994) has become the prototype of a merging cluster. It has been observed by every modern X-ray observatory, and a series of papers in the last few years,

¹Also IKI, Moscow, Russia

based on these data have established that there is evidence of a merger in progress. Fabricant (1986) used the X-ray imaging data obtained by the Einstein IPC and interpreted the elongated shape of the surface brightness distribution as merging subclusters. Henriksen (1986) fit a β -model to the Einstein imaging data to obtain the gas density profile and utilized a polytropic relationship to predict gas temperature profiles which were then constrained by the HEAO1-A2 spectra. These data required non-isothermality in the gas and were consistent with a monotonically decreasing temperature profile with the hottest material in the center and the coolest on the outside. In 1993, Henriksen analyzed HEAO1-A2 spectra along with Einstein IPC and SSS spectra and found further evidence of non-isothermality in the gas and that the data were also consistent with a simpler two-component model including a very hot and a cooler gas. The lack of combined spatial and spectral resolution in the data made the location of the thermal components ambiguous. Henry and Briel (1995, hereafter HB) analyzed ROSAT PSPC data in the energy band 0.5–2 keV, which provided a high quality image of the cluster as well as spectral constraints. These authors found that the hot gas is in the general vicinity of the North-West (NW) galaxy clump identified by Zabludoff and Zaritsky (1995), while the cluster brightness peak, in the vicinity of the South-East (SE) galaxy group, has a lower temperature as does the outer region of the cluster atmosphere.

Hydrodynamical simulations of the effect of the subcluster merger on the intracluster medium predict the existence of relatively long-lived spatial temperature variations in the post-merger cluster gas (e.g., Schindler & Müller 1993; Roettiger, Burns & Loken 1993; Evrard et al. 1996). ASCA data have spectral and spatial resolution combined with a broad energy band which is sufficient to test these predictions and determine the evolutionary stage of clusters, and put constraints on the physics of cluster mergers. In this Letter, we present an analysis of spatially resolved spectra obtained by ASCA of A754, which have provided temperature and abundance maps of the cluster.

2. Observations and Analysis

A754 was observed by ASCA (Tanaka et al. 1994) for 15–18 ks with the SIS (most of it in the 4-CCD mode which covers a square $22' \times 22'$ field) and for 21 ks with the GIS. We used all four ASCA detectors in the analysis. For reconstruction of the cluster gas temperature map, the scheme from Markevitch (1996, and references therein) has been used. It consists of simultaneous fitting the temperature in all chosen image regions, taking into account the ASCA mirror scattering. The mirror Point Spread Function was modeled using Cyg X-1 data for energies above 2 keV (Takahashi et al. 1995). For the energies 1.5–2 keV where these data are inaccurate, the PSF data from the 2–3 keV interval were used after the appropriate correction for the energy dependence of the GIS spatial resolution. Including this energy interval in the analysis did not change the best-fit values noticeably while improving statistics. We chose to use only energies above 1.5 keV for the spatially-resolved analysis to avoid further extrapolation of the PSF model, while using all energies above 0.5 keV in the overall spectrum analysis. The PSF uncertainty of 15% (1σ) was included in the confidence interval calculation. There are no bright sources in the vicinity of A754 so a possible stray light contribution (Ishisaki 1996) is unimportant for our analysis. The background was modeled using the blank field observations normalized according to their exposures, and an uncertainty of such normalization of 20% was also included. A ROSAT PSPC image of the cluster was used as a brightness template as in Markevitch (1996). The data from GIS and SIS were binned in 8 and 7 wide spectral bins, respectively. The poorly calibrated 2–2.5 keV interval was excluded; including it didn't change the best-fit values significantly but made χ^2 worse. Iron abundance and the absorbing column were assumed constant at their Ginga and Galactic values, respectively, and varying them didn't change the best-fit temperatures significantly.

The PSF effects are most important for the regions of low relative surface brightness, while in many cases one can get a meaningful temperature estimate for the brightness peak regions by fitting its spectrum directly without accounting for the added scattered flux. We have performed such fits including lower energies for several regions, to cross-check the results of the general method.

3. Results: Temperature and Abundance Maps

The GIS-measured luminosity of A754 in the 0.5–10 keV band is $2.4 \times 10^{44} h^{-2} \text{ ergs s}^{-1}$, where $H_0 = 100h \text{ km s}^{-1} \text{ Mpc}^{-1}$. The emission-weighted temperature using all four detectors is $8.5 \pm 0.5 \text{ keV}$ (9 keV using the energy interval of 1.5–11 keV used for the temperature map), in agreement with the 90% confidence range for GINGA, $8.6 \pm 0.5 \text{ keV}$ and HEAO1-A2, 7.8–9.0 keV. The abundance, 0.26 ± 0.05 , is derived fitting a single component Raymond and Smith model with Xspec utilizing the Solar ratios in Allen (1973). It is consistent with the Ginga value of 0.27 ± 0.04 , confirming that A754 has a metallicity typical of a rich cluster. The HEAO1-A2 values are taken from Henriksen (1993) and the Ginga results from Arnaud (1994).

A two-dimensional temperature map is shown in Fig. 1, in which the ASCA temperatures (grayscale) are overlaid on the ROSAT PSPC surface brightness contours. The regions in which the temperatures were reconstructed are nine 5 arcmin boxes in the inner part, and four segments of the 16 arcmin-radius circle in the outer part. As anticipated for a cluster undergoing merger, the temperature distribution is significantly non-uniform: regions 1, 4, 7 and 8 along the cluster axis, are hotter than the cluster average at a greater than 90% confidence, while regions 10 and 13 on the outside are significantly cooler. The obtained temperatures generally agree with HB’s ROSAT PSPC values within the much larger ROSAT errors. Exceptions are our regions 6 and 12 whose ASCA temperatures are consistent with the average, while HB’s values for approximately the same regions are higher, however at a low statistical significance. In the region approximately corresponding to our region 2+3 which includes the cluster brightness peak, HB detected a significantly lower temperature than ours. We have looked into the disagreement and found that when a smaller region centered on the PSPC brightness peak is considered and the lower energies are included in the analysis (without the PSF correction, see section above), our best-fit temperature is lower, see Table 1. This indicates that the spectrum in this region may be multicomponent, and the origin of the discrepancy is in the higher sensitivity of PSPC to the lower-temperature component while ASCA is picking the higher-temperature component. We have also made an estimate without the PSF correction for some other selected regions. The region centered on the SE galaxy group (Fabricant et al. 1986; Zabludoff & Zaritsky 1995), 3’ to the South from the PSPC peak, also appears cooler. For a circle centered on the NW galaxy group (about 4’ westward from the center of the region 8 in the temperature map), the simple analysis yields a high temperature, 11.5 keV, in agreement with that from the full analysis. It may be worth noticing that using the concentric annuli around the cluster center, both with and without correcting for the PSF, would conceal the complex temperature structure of this cluster (see Table 1) within the central 20’. The azimuthally averaged temperature appears to drop with radius beyond $r \sim 10' \simeq 0.4 h^{-1} \text{ Mpc}$, as seen from Fig. 1.

For the first time we have attempted to reconstruct a two-dimensional abundance map of this cluster. Abundance variations may be an important diagnostic in assessing gas mixture expected from the turbulence generated by the subcluster merger. To derive the abundances in the regions for which the temperatures have been obtained while avoiding fitting an unmanageable number of free parameters, we have fixed the temperatures at their best-fit values obtained with constant abundances. It is a justifiable thing to do because the ASCA energy resolution and energy coverage are sufficient to separate fitting of the temperature

and the abundance. The resulting abundances in the individual regions are given in Table 2. The abundance constraints are poor, due to the insufficient statistics of the ASCA observation, with most of the abundances consistent with the average within the 68% confidence intervals. We will return to the abundances in the section below.

4. Discussion

Summarizing the findings of ROSAT and ASCA, A754 is significantly non-isothermal. There is a ridge of hot gas located approximately alongside the cluster elongation axis, with the highest temperatures in the area of the NW galaxy concentration. The X-ray brightness peak, elongated in the direction perpendicular to the cluster axis, contains gas which is significantly cooler than the cluster average, as are the cluster outskirts toward North and East. The question which we would like to address using our derived temperature distribution is the evolutionary history of A754. Detailed hydrodynamic simulations of cluster mergers (e.g., Schindler & Müller 1993; Roettiger, Burns & Loken 1993; Pearce et al. 1994) predict that as a result of a recent or ongoing merger, the cluster should have a strongly peaked temperature distribution with the highest temperature at the site of the subcluster collision, accompanied by hot lobes perpendicular to the collision axis. Briel & Henry (1994) reported on the detection of such hot lobes in another cluster, A2256, using ROSAT PSPC. However, their existence was not confirmed by ASCA (Markevitch 1996), who also failed to detect the central temperature peak in that cluster. Using ASCA data, Arnaud et al. (1994) and Markevitch et al. (1994) reported irregular temperature structure in Perseus and in A2163, respectively, attributing it to the merger effects, although the former have ignored the PSF scattering while the statistical significance of the latter result was marginal. A754 remains the only cluster for which there is a significant and unambiguous indication of the irregular temperature structure expected in a merger, providing the first possibility to compare it with theoretical predictions.

If one assumes, in line with all previous studies of A754, that the merger in this cluster proceeds in the direction of the cluster elongation, one expects to find a temperature structure quite different from what is observed. We offer two possible explanations for this. One is that unlike in the simulations which considered highly supersonic ($\sim 3000 \text{ km s}^{-1}$) mergers, the subcluster collision velocity is low and the post-shock gas temperature, proportional to the upstream shock velocity squared, is not significantly high. Analysis of optical data indicates that mergers may likely occur at a lower velocity, for example, $\sim 500 \text{ km s}^{-1}$ for A98 (Beers, Geller & Huchra 1982) and $\sim 1500 \text{ km s}^{-1}$ for A3395 (Henriksen & Jones 1996). The line-of-sight velocity difference of the galaxy clumps in A754 is very low, about 100 km s^{-1} (Zabludoff & Zaritsky 1995) though application of a simple dynamical model by these authors results in a post-merger, relative velocity of $\sim 2000 \text{ km s}^{-1}$. However, the observed heating along the cluster axis remains to be explained in this scenario.

A more plausible explanation is a merger with a non-zero impact parameter. Evrard et al. (1996) show a simulation of a merger which is reprinted here as our Fig. 2 and is strikingly similar to A754. In this scenario, the merger proceeds in the image plane with the subunits infalling from North and South with the impact parameter $\sim 0.5 h^{-1} \text{ Mpc}$, as shown by the gas velocity arrows in the left panel of Fig. 2 (gas is expected to drag behind the dark matter during a merger.) The hottest region is at the site of the NW group penetrating the larger subunit, and the brightness elongation to the South is the tail of this group. The plume of cool gas at the X-ray brightness peak is the stripped atmosphere, and perhaps even a cooling flow, belonged to the subunit associated with the SE galaxy group, its elongation (more clearly seen in the full resolution ROSAT image presented in HB) pointing in the direction of that group’s infall.

The fact that the cold gas still exists in the cluster may indicate that the merger has not proceeded very far and this is the first encounter of the subclusters. It is therefore interesting to see if any large-scale elemental abundance differences exist, indicating that the gas belonged to different subclusters and still retains its identity (if the subunit’s abundances have been different). We have averaged the abundances over the North-East (regions 2, 3, 6, 10, 13 in Fig. 1) and the South-West (regions 4, 7, 8, 11, 12) areas of the cluster associated with the two infalling subunits (excluding the regions 1, 5, 9), and found the abundances of 0.45 ± 0.12 and 0.29 ± 0.13 (68% intervals), respectively. They are consistent within the statistical errors, although there is a hint of difference and it would be interesting to measure them with a better accuracy.

To conclude, using ASCA data, we have found a prominent structure in the temperature map of A754 and put some constraints on the abundances in the different cluster regions. All of the evidence, including the X-ray image and the optical galaxy distribution, is consistent with a non-head-on merger proceeding with high velocity in the image plane. With such favorable viewing angle and the merger stage, A754 is an ideal laboratory to test various evolutionary scenarios.

MJH gratefully acknowledges support from NASA grant NAG5-2529 and the hospitality of the ASCA GOF at GSFC where part of the analysis was completed. MM was supported by NASA grants NAG5-2526 and NAG5-1891.

REFERENCES

- Allen, C.W. 1973, *Astrophysical Quantities*, 3rd ed., London: Athlone Press
- Arnaud, M. 1994, in *Cosmological Aspects of X-ray Clusters of Galaxies*, ed. W.C. Seitter (Dordrecht: Kluwer), 197
- Arnaud, K., et al. 1994, *ApJ*, 436, 67L
- Beers, T., Geller, M., & Huchra, J. 1982, *ApJ*, 257, 23
- Bird, C. M. 1994, *AJ*, 107, 1637
- Evrard, A. E., Metzler, C. A., & Navarro, J. F. 1996, *ApJ*, in press (preprint astro-ph/9510058)
- Fabricant, D., Beers, T., Geller, M., Gorenstein, P., Huchra, J., & Kurtz, M. 1986, *ApJ*, 308, 530
- Henriksen, M. 1986, PhD Thesis, University of Maryland
- Henriksen, M. 1993, *ApJ*, 414, L5
- Henriksen, M., & Jones, C. 1996, *ApJ* (in press)
- Henry, J., & Briel, U. 1995, *ApJ*, 443, L9 (HB)
- Ishisaki, Y., 1996, PhD thesis, University of Tokyo
- Markevitch, M., Yamashita, K., Furuzawa, A., & Tawara, Y. 1994, *ApJ*, 436, L71
- Markevitch, M. 1996, *ApJ Letters* (in press); preprint astro-ph/9604149
- Pearce, F. R., Thomas, P. A., & Couchman, H. M. P. 1994, *MNRAS*, 268, 953
- Roettiger, K., Burns, J., & Loken, C. 1993, *ApJ*, 407, L53
- Schindler, S., & Müller, E., 1993, *A&A*, 272, 137
- Takahashi, T., et al. 1995, *ASCA Newsletter No. 3*, NASA/GSFC
- Tanaka, Y., Inoue, H., & Holt, S. S. 1994, *PASJ* 46, L37
- Zabludoff, A., & Zaritsky, D. 1995, *ApJ*, 447, L21

| Region | r , arcmin | kT_e , keV | Abundance |
|-----------------|--------------|----------------------|------------------------|
| PSPC peak | 1.3 | $6.1^{+1.1}_{-0.8}$ | $0.35^{+0.24}_{-0.24}$ |
| SE Galaxy Clump | 1.8 | $6.6^{+1.2}_{-1.0}$ | $0.35^{+0.35}_{-0.35}$ |
| NW Galaxy Clump | 2.3 | $11.5^{+3.5}_{-2.2}$ | $0.35^{+0.39}_{-0.35}$ |
| Annulus 1 | 0–3.5 | $8.6^{+0.5}_{-0.6}$ | $0.28^{+0.07}_{-0.07}$ |
| Annulus 2 | 3.5–7.5 | $8.3^{+0.3}_{-0.4}$ | $0.25^{+0.02}_{-0.05}$ |
| Annulus 3 | 7.5–10.8 | $8.7^{+0.6}_{-0.5}$ | $0.27^{+0.07}_{-0.07}$ |

Table 1.—Results from modeling regions without taking account of PSF, including all energies. Errors are 68%. The values for the brightness peaks should be reasonably close to the actual values, while values for the annuli may be affected by the PSF scattering and are given here for illustration only. The annuli are centered approximately on the region 5 of Fig. 1.

| Region | Abundance | 68% Interval |
|--------|-----------|--------------|
| 1 | 0.60 | 0.1–0.9 |
| 2 | 0.31 | 0.26–0.46 |
| 3 | 0.63 | 0.1–0.8 |
| 4 | 0.00 | 0–0.3 |
| 5 | 0.31 | 0.18–0.41 |
| 6 | 0.12 | 0–0.6 |
| 7 | 0.10 | 0–1.2 |
| 8 | 0.28 | 0–0.3 |
| 9 | 0.00 | 0–0.3 |
| 10 | 0.89 | 0.5–1.3 |
| 11 | 0.39 | 0.2–0.9 |
| 12 | 0.32 | 0.1–0.5 |
| 13 | 0.36 | 0.1–0.6 |

Table 2.—Iron abundances in the regions of Fig. 1. Temperatures were kept fixed at their best-fit values obtained for the uniform best-fit abundance (see text).

color

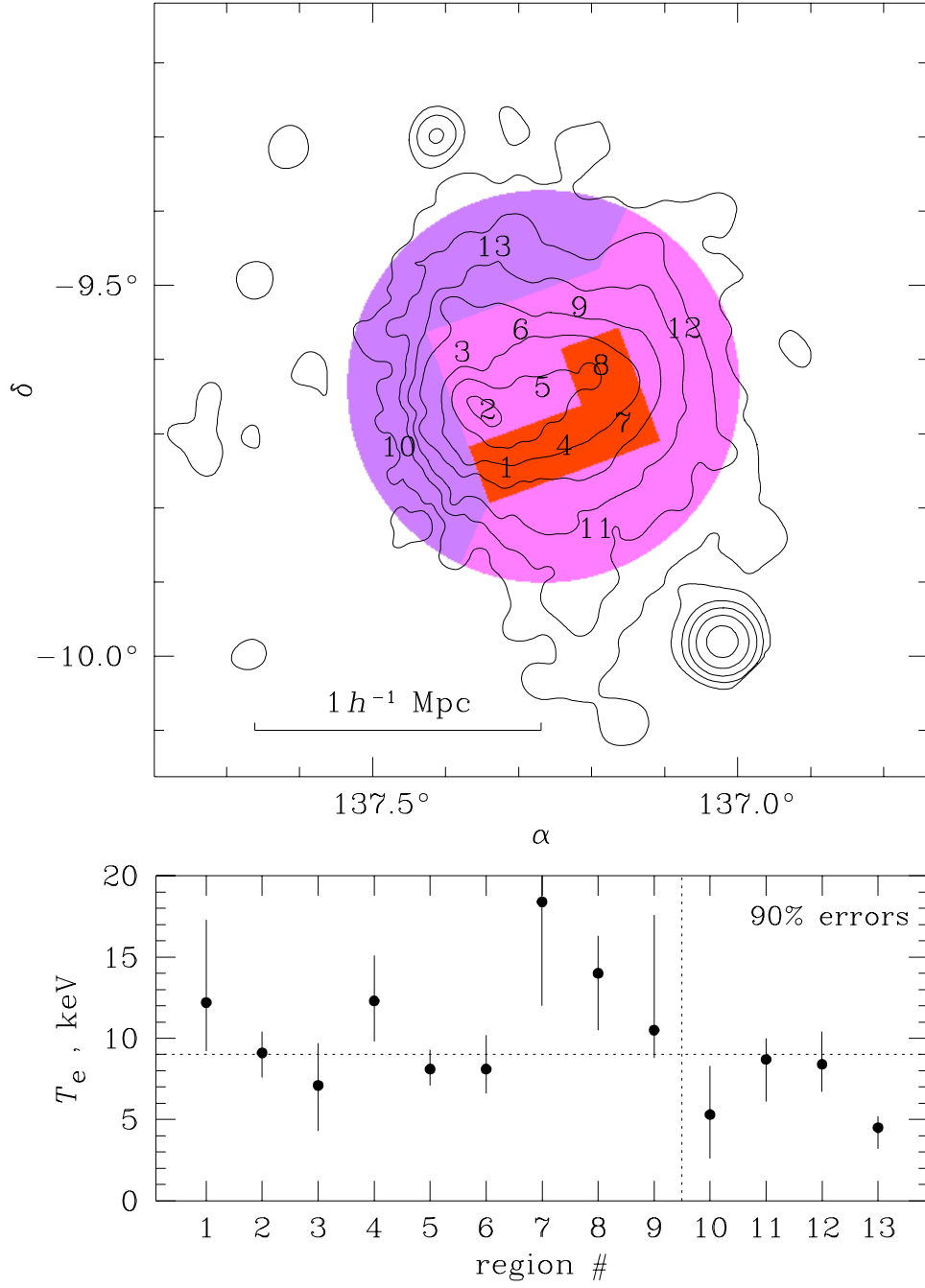


Fig. 1.—Temperature map of A754. Contours show the ROSAT brightness and color shows ASCA temperatures of the cluster regions marked by their numbers in the lower panel. The regions are nine 5 arcmin boxes in the inner part and segments of the 16 arcmin-radius annulus in the outer part. The lower panel shows temperature values with their one-parameter 90% confidence intervals for each region. Dashed line is drawn at the average cluster temperature (9.0 keV) obtained using the same energy band, 1.5–11keV.

grayscale

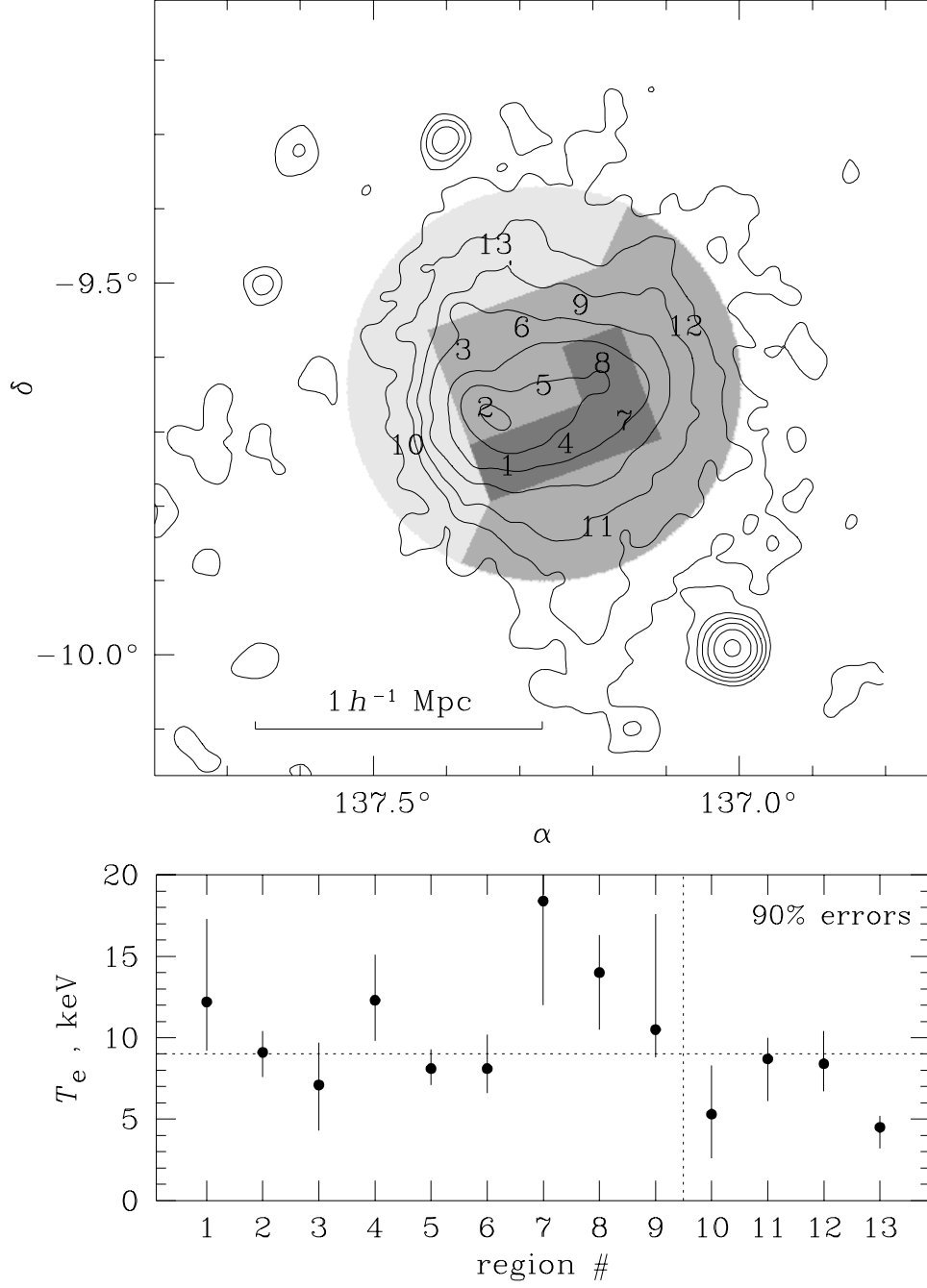


Fig. 1.—Temperature map of A754. Contours show the ROSAT brightness and grayscale shows ASCA temperatures (darker is hotter) of the cluster regions marked by their numbers in the lower panel. The regions are nine 5 arcmin boxes in the inner part and segments of the 16 arcmin-radius annulus in the outer part. The lower panel shows temperature values with their one-parameter 90% confidence intervals for each region. Dashed line is drawn at the average cluster temperature (9.0 keV) obtained using the same energy band, 1.5–11keV.

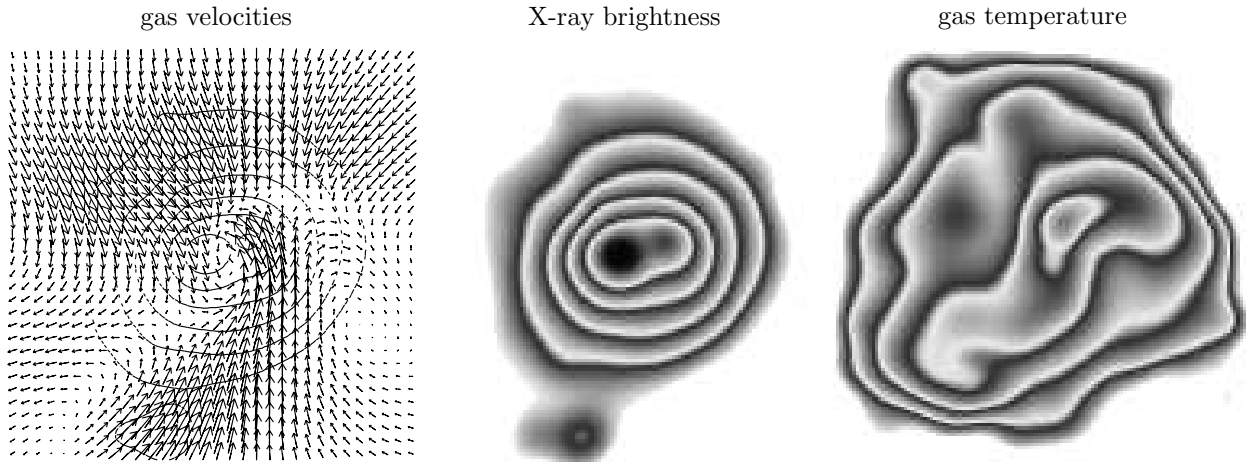


Fig. 2.—A simulated cluster from Evrard et al. (1996), rotated to match the orientation of A754 (included with permission from A. Evrard.) The brightness and temperature maps closely resemble those of A754 (Fig. 1). Arrows in the left panel denote cluster gas velocities, overlaid on the X-ray brightness contours. The gas generally drags behind the dark matter during a merger. The grayscale bands in the right panel which shows the X-ray emissivity-weighted temperature, are spaced logarithmically by $10^{0.2}$. The merger is proceeding in the North-South direction with a non-zero impact parameter, which we propose as a scenario for A754.